

Neutron-rich hypernuclei: ${}^6_{\Lambda}\text{H}$ and beyond

A. Gal^{a,*}, D.J. Millener^b

^a*Racah Institute of Physics, The Hebrew University, 91904 Jerusalem, Israel*

^b*Physics Department, Brookhaven National Laboratory, Upton, NY 11973, USA*

Abstract

Recent experimental evidence presented by the FINUDA Collaboration for a particle-stable ${}^6_{\Lambda}\text{H}$ has stirred renewed interest in charting domains of particle-stable neutron-rich Λ hypernuclei, particularly for unbound nuclear cores. We have studied within a shell-model approach several neutron-rich Λ hypernuclei in the nuclear p shell that could be formed in (π^-, K^+) or in (K^-, π^+) reactions on stable nuclear targets. Hypernuclear shell-model input is taken from a theoretically inspired successful fit of γ -ray transitions in p -shell Λ hypernuclei which includes also $\Lambda N \leftrightarrow \Sigma N$ coupling ($\Lambda\Sigma$ coupling). The particle stability of ${}^6_{\Lambda}\text{H}$ is briefly discussed. Predictions are made for binding energies of ${}^9_{\Lambda}\text{He}$, ${}^{10}_{\Lambda}\text{Li}$, ${}^{12}_{\Lambda}\text{Be}$, ${}^{14}_{\Lambda}\text{B}$. None of the large effects conjectured by some authors to arise from $\Lambda\Sigma$ coupling is borne out, neither by these realistic p -shell calculations, nor by quantitative estimates outlined for heavier hypernuclei with substantial neutron excess.

Keywords:

hypernuclei, effective interactions in hadronic systems, shell model

PACS: 21.80.+a, 21.30.Fe, 21.60.Cs

1. Introduction

Dalitz and Levi Setti, fifty years ago [1], discussed the possibility that Λ hyperons could stabilize particle-unstable nuclear cores of Λ hypernuclei and thus allow studies of neutron-rich baryonic systems beyond the nuclear drip line. The Λ 's effectiveness to enhance binding is primarily connected with the Pauli principle from which it is exempt, allowing it to occupy the lowest

*Corresponding author: Avraham Gal, avragal@vms.huji.ac.il

$1s_\Lambda$ orbital. Several unbound-core Λ hypernuclei have since been identified in emulsion work, the neutron richest of which is $^8_\Lambda\text{He}$ [2]. Of particular interest is the recent FINUDA evidence for a particle-stable $^6_\Lambda\text{H}$ hypernucleus produced in the $^6\text{Li}(K^-_{\text{stop}}, \pi^+)$ reaction [3, 4]. In distinction from the well-established hyper-hydrogen isotopes $^3,4_\Lambda\text{H}$, the ^5H nuclear core of $^6_\Lambda\text{H}$ is unbound, and its neutron-proton excess ratio $(N - Z)/(N + Z) = 0.6$ is unsurpassed by any stable or Λ -stabilized core nucleus. The $^6_\Lambda\text{H}$ hypernucleus was highlighted by Akaishi [5] as a testground for the significance of $\Lambda\Sigma$ coupling in Λ hypernuclei, spurred by the role it plays in s -shell hypernuclei [6, 7] and by the far-reaching consequences it might have for dense neutron-star matter with strangeness [8]. In the present work, and as a prelude to its main theme, we discuss the particle stability of $^6_\Lambda\text{H}$ from the point of view of the shell model, focusing on $\Lambda\Sigma$ coupling contributions and making comparisons with other calculations and with the FINUDA experimental claim.

The purpose of this Letter is to provide shell-model predictions for other neutron-rich Λ hypernuclei that could be reached at J-PARC in (π^-, K^+) or (K^-, π^+) reactions on stable nuclear targets in the p shell. A missing-mass $^6\text{Li}(\pi^-, K^+)$ spectrum from J-PARC in-flight experiment E10 [9] is under study at present, aimed at assessing independently FINUDA's evidence for a particle-stable $^6_\Lambda\text{H}$ hypernucleus. In the present analysis, based on extensive hypernuclear shell-model calculations [10], we use $0s_\Lambda 0p_N$ effective interactions with matrix elements constrained by the most comprehensive set of hypernuclear γ -ray measurements by Tamura et al. [11]. Included explicitly are also $0s_\Lambda 0p_N \leftrightarrow 0s_\Sigma 0p_N$ effective interactions based on the $0s_Y 0s_N$ G -matrix interactions ($Y = \Lambda, \Sigma$) used in the comprehensive s -shell hypernuclear calculations of Ref. [6]. The methodology of this shell-model analysis is briefly reviewed in Section 2, following which we discuss $^6_\Lambda\text{H}$ in Section 3 and then, in Section 4, the neutron-rich hypernuclei that can be produced on stable nuclear targets in the nuclear p shell. Ground-state binding energies and doublet splittings are evaluated. Also outlined in this section is a shell-model evaluation of $\Lambda\Sigma$ coupling effects in heavier hypernuclei with larger neutron excess, such as $^{49}_\Lambda\text{Ca}$ and $^{209}_\Lambda\text{Pb}$, demonstrating that the increase in neutron excess is more than compensated by the decrease of the $\Lambda\Sigma$ coupling matrix elements with increasing orbital angular momentum ℓ_N of the valent nucleon configurations involved in the coherent coupling approximation. We thus conclude that none of the large effects conjectured by Akaishi et al. [5, 12, 13] to arise from $\Lambda\Sigma$ coupling is borne out in realistic calculations.

2. Shell-model methodology

The ΛN effective interaction

$$V_{\Lambda N} = \bar{V} + \Delta \vec{s}_N \cdot \vec{s}_\Lambda + S_\Lambda \vec{l}_N \cdot \vec{s}_\Lambda + S_N \vec{l}_N \cdot \vec{s}_N + T S_{N\Lambda}, \quad (1)$$

where $S_{N\Lambda} = 3(\vec{\sigma}_N \cdot \vec{r})(\vec{\sigma}_\Lambda \cdot \vec{r}) - \vec{\sigma}_N \cdot \vec{\sigma}_\Lambda$, is specified here by its $0s_\Lambda 0p_N$ spin-dependent matrix elements within a $0\hbar\omega$ shell-model space. The same parametrization applies also to the $\Lambda\Sigma$ coupling interaction and the ΣN interaction for both isospin 1/2 and 3/2, with an obvious generalization to account for the isospin 1 of the Σ hyperon. The detailed properties of the ΣN interaction parameters hardly matter in view of the large energy denominators of order $M_\Sigma - M_\Lambda \approx 80$ MeV with which they appear. To understand the effects of the $\Lambda\Sigma$ coupling interaction, it is convenient to introduce an overall isospin factor $\sqrt{4/3} \vec{t}_N \cdot \vec{t}_{\Lambda\Sigma}$, where $\vec{t}_{\Lambda\Sigma}$ converts a Λ to Σ in isospace. Matrix elements of the ΛN effective interaction (1) and of the $\Lambda\Sigma$ coupling interaction are listed in Table 1. The ΛN matrix elements were fitted to a wealth of hypernuclear γ -ray measurements [14], resulting in values close to those derived from the YN interaction models NSC97 [15]. The $\Lambda\Sigma$ matrix elements are derived from the same NSC97 models used to construct $0s_Y 0s_N$ G -matrix interactions in s -shell Λ hypernuclear calculations [6]. By limiting here the ΣN model-space to $0s_\Sigma 0p_N$, in parallel to the $0\hbar\omega$ $0s_\Lambda 0p_N$ model-space used for ΛN , we maintain the spirit of Akaishi's *coherent* approximation¹ which is designed to pick up the strongest $\Lambda\Sigma$ matrix elements.

It is clear from Table 1 that the only significant $\Lambda\Sigma$ interaction parameters are $\bar{V}_{\Lambda\Sigma}$ and $\Delta_{\Lambda\Sigma}$, in obvious notation. The first one is associated with diagonal matrix elements of the spin-independent part of the $\Lambda\Sigma$ interaction, viz.

$$\langle (J_N T, s_\Lambda) JT | V_{\Lambda\Sigma} | (J_N T, s_\Sigma) JT \rangle = \sqrt{4/3} \sqrt{T(T+1)} \bar{V}_{\Lambda\Sigma}. \quad (2)$$

This part preserves the nuclear core, specified here by its total angular momentum J_N and isospin T , with matrix elements that bear resemblance to the Fermi matrix elements in β decay of the core nucleus. Similarly, the

¹By *coherent* we mean $0s_\Lambda n l_N \leftrightarrow 0s_\Sigma n l_N$ coupling that preserves hyperon and nucleon orbits, where $n l_N$ denotes the nuclear orbits occupied in the core-nucleus wavefunction. For the $A = 4$ hypernuclei considered by Akaishi, this definition reduces to the assumption that the Λ and Σ , both in their $0s$ orbits, are coupled to the *same* nuclear core state. The parameters listed in the last line of Table 1 contribute almost 0.6 MeV to the binding of ${}^4_\Lambda\text{H}(0^+_{\text{g.s.}})$ and more than 0.5 MeV to the excitation energy of ${}^4_\Lambda\text{H}(1^+_{\text{exc.}})$.

Table 1: $0s_\Lambda 0l_N \leftrightarrow 0s_Y 0l_N$ matrix elements from Ref. [10] (in MeV). \bar{V} and Δ are the spin-average and difference of the triplet and singlet central matrix elements. For the $s_N^3 s_Y$ hypernuclei, the $\Lambda\Sigma$ coupling matrix elements are $v(0_{\text{g.s.}}^+) = \bar{V}_{\Lambda\Sigma}^{0s} + \frac{3}{4}\Delta_{\Lambda\Sigma}^{0s}$ and $v(1_{\text{exc.}}^+) = \bar{V}_{\Lambda\Sigma}^{0s} - \frac{1}{4}\Delta_{\Lambda\Sigma}^{0s}$, with downward energy shifts $\delta E_\downarrow(J^\pi) \approx v^2(J^\pi)/(80 \text{ MeV})$.

Y	$0l_N$	\bar{V}	Δ	S_Λ	S_N	T
Λ ($A \leq 9$)	$0p_N$		0.430	-0.015	-0.390	0.030
Λ ($A \geq 10$)	$0p_N$		0.330	-0.015	-0.350	0.024
Σ	$0p_N$	1.45	3.04	-0.09	-0.09	0.16
Σ	$0s_N$	2.96	5.09	—	—	—

spin-spin part of the $\Lambda\Sigma$ interaction associated with the matrix element $\Delta_{\Lambda\Sigma}$ involves the operator $\sum_j \vec{s}_{Nj} \vec{t}_{Nj}$ for the core, connecting core states with large Gamow-Teller transition matrix elements as emphasized recently by Umeya and Harada in their study of the ${}^7\text{--}^{10}_\Lambda\text{Li}$ isotopes [16].

Finally, the ΛN spin-independent matrix element \bar{V} is not specified in Table 1 because it is not determined by fitting hypernuclear γ -ray transitions. Its value is to be deduced from fitting absolute binding energies. Suffice to say that \bar{V} assumes values of $\bar{V} \approx -1.0 \pm 0.1 \text{ MeV}$. We consider it as part of a mean-field description of Λ hypernuclei, consistent with the observation that on the average throughout the p shell $B_\Lambda(A)$ increases by about 1 MeV upon increasing A by one unit.

3. ${}^6_\Lambda\text{H}$

The low-lying spectrum of ${}^6_\Lambda\text{H}$ consists of a $0_{\text{g.s.}}^+$ and $1_{\text{exc.}}^+$ states which, disregarding the two p -shell neutrons known from ${}^6\text{He}$ to couple dominantly to $L = S = 0$, are split in ${}^4_\Lambda\text{H}$ by $1.08 \pm 0.02 \text{ MeV}$ [17]. These states in ${}^6_\Lambda\text{H}$ are split by $1.0 \pm 0.7 \text{ MeV}$, judging by the systematic difference noted in the FINUDA experiment [3, 4] between the mass values $M({}^6_\Lambda\text{H})$ from production and decay, as shown in Fig. 1. The observation of ${}^6_\Lambda\text{H} \rightarrow \pi^- + {}^6\text{He}$ weak decay in the FINUDA experiment implies that ${}^6_\Lambda\text{H}$ is particle-stable, with $2n$ separation energy $B_{2n}({}^6_\Lambda\text{H}_{\text{g.s.}}) = 0.8 \pm 1.2 \text{ MeV}$. A phenomenological shell-model estimate cited in Ref. [4] yields a similar value:

$$B_{2n}({}^6_\Lambda\text{H}) = B_{2n}({}^5\text{H}) + [B_\Lambda({}^7_\Lambda\text{He}) - B_\Lambda({}^5_\Lambda\text{He})] = (-1.7 \pm 0.3) + (2.56 \pm 0.25) \text{ MeV}, \quad (3)$$

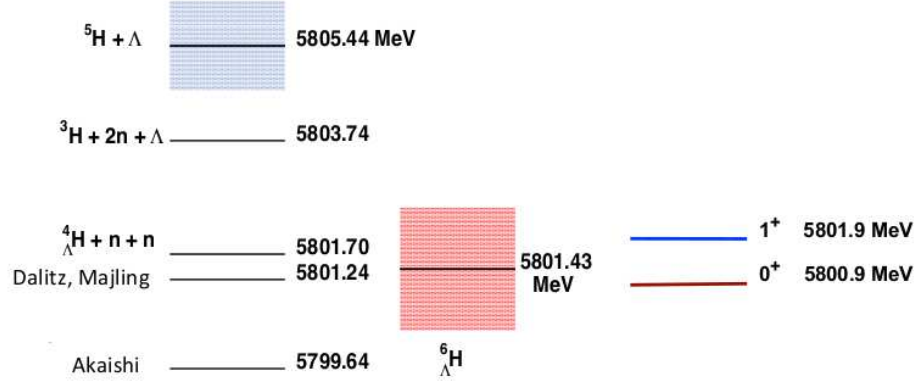


Figure 1: ${}^6_{\Lambda}\text{H}$ binding energy diagram adapted from Ref. [4], with thresholds marked on its upper-left side and theory predictions beneath [1, 12]. The location of the ${}^5\text{H}$ resonance vs. the ${}^3\text{H}+2n$ threshold, with the (blue) hatched box denoting its width, is taken from Ref. [18]. The (red) shaded box represents the error on the mean production and decay mass value obtained from the three FINUDA events assigned to ${}^6_{\Lambda}\text{H}$, whereas the positions of the $1^+_{\text{exc.}}$ and $0^+_{\text{g.s.}}$ levels marked on the right-hand side are derived separately from production and decay, respectively. We thank Elena Botta for providing this figure.

accepting the ${}^5\text{H}$ mass determination from Ref. [18] and extracting the Λnn interaction, including $\Lambda\Sigma$ coupling contributions, from the difference of Λ binding energies within the square bracket. It is based on observing that the Λnn configuration for the two p -shell neutrons in ${}^6_{\Lambda}\text{H}$ is identical with that in ${}^7_{\Lambda}\text{He}$ (recently produced at Jlab [19]). The corresponding phenomenological shell-model estimate for $B_{\Lambda}({}^6_{\Lambda}\text{H})$ is

$$B_{\Lambda}({}^6_{\Lambda}\text{H}) = B_{\Lambda}({}^4_{\Lambda}\text{H}) + [B_{\Lambda}({}^7_{\Lambda}\text{He}) - B_{\Lambda}({}^5_{\Lambda}\text{He})] = (2.04 \pm 0.04) + (2.56 \pm 0.25) \text{ MeV}. \quad (4)$$

These estimates need to be revised on two counts, as follows.

First, one notes that the nuclear s shell is not closed in ${}^6_{\Lambda}\text{H}$, in distinction from all other neutron-rich Λ hypernuclei considered in the present work, so that the $\Lambda\Sigma$ coupling contribution in ${}^6_{\Lambda}\text{H}$ is not the sum of the separate contributions from the s shell through ${}^4_{\Lambda}\text{H}$ and from the p shell through ${}^7_{\Lambda}\text{He}$. For an s^3p^2 core of ${}^6_{\Lambda}\text{H}$, with [32] spatial symmetry and $T = 3/2$, the coherent $\Lambda\Sigma$ coupling diagonal matrix element is $\sqrt{5/9}v(J^{\pi}) + \sqrt{20/9}\bar{V}_{\Lambda\Sigma}^{0p}$ for $J^{\pi} = 0^+, 1^+$, where $v(J^{\pi})$ is the corresponding $A = 4$ matrix element (see caption to Table 1), with no contribution from $\Delta_{\Lambda\Sigma}^{0p}$ because the two p -shell neutrons have Pauli spin zero. $\Lambda\Sigma$ contributions to the binding energies

of Λ hypernuclei involved in the shell model evaluation of the ${}^6_\Lambda\text{H}$ doublet levels $0^+_{\text{g.s.}}$ and $1^+_{\text{exc.}}$, calculated for the interaction specified in Table 1, are listed in Table 2. Whereas ${}^4_\Lambda\text{H}$ admits only a diagonal matrix-element contribution, the p -shell hypernuclei admit both diagonal as well as nondiagonal matrix-element contributions, with the listed diagonal ones dominating. It is also seen that ${}^6_\Lambda\text{H}(0^+_{\text{g.s.}})$ gains 149 keV and ${}^6_\Lambda\text{H}(1^+_{\text{exc.}})$ gains 42 keV binding above the sum of separate contributions from ${}^4_\Lambda\text{H}$ and ${}^7_\Lambda\text{He}$ inherent in the phenomenological shell-model approach.

Table 2: $\Lambda\Sigma$ contributions (in keV) to binding energies of Λ hypernuclei involved in shell-model considerations of ${}^6_\Lambda\text{H}$ stability.

J^π	${}^4_\Lambda\text{H}$ diag.=tot.	${}^7_\Lambda\text{He}(\frac{1}{2}^+_{\text{g.s.}})$ diag.	${}^7_\Lambda\text{He}(\frac{1}{2}^+_{\text{g.s.}})$ total	${}^6_\Lambda\text{H}$ diag.	${}^6_\Lambda\text{H}$ total
0^+	574	70	98	650	821
1^+	36	70	98	146	176

A more important reason for revising the phenomenological shell-model estimate is the reduction of shell-model matrix elements that involve a spatially extended p -shell neutron in ${}^6_\Lambda\text{H}$ ($B_{2n} \lesssim 0.8$ MeV) relative to matrix elements that involve a more compact p -shell neutron in ${}^7_\Lambda\text{He}$ ($B_n \sim 3.0$ MeV). The average neutron separation energy for ${}^6_\Lambda\text{H}$ is close to $B_n({}^6_\Lambda\text{He}) = 0.26 \pm 0.14$ MeV. From $B_\Lambda({}^6_\Lambda\text{He})$ and using our shell-model estimates for the spin-dependent and $\Lambda\Sigma$ coupling contributions, we deduce $\bar{V} \sim -0.8$ MeV and a similar reduction of roughly 20% in other $0s_\Lambda 0p_N$ interaction matrix elements, which in turn gives $B_\Lambda({}^6_\Lambda\text{H}) \sim B_\Lambda({}^4_\Lambda\text{H}) - 2\bar{V} + \delta = 2.04 + 1.60 + 0.34 = 3.98$ MeV, where $\delta = 0.34$ MeV accounts for the renormalized ΛN spin-dependent contribution and the $\Lambda\Sigma$ contribution above that already included in $B_\Lambda({}^4_\Lambda\text{H})$. Because the s^3p^2 core for ${}^6_\Lambda\text{He}$ will be more spatially extended than the α -particle core for the He hypernuclei, a few-body calculation such as that of Hiyama et al. [20], discussed below, is required. We therefore consider the present shell-model estimate, listed in Table 3 below, as an upper bound for $B_\Lambda({}^6_\Lambda\text{H})$.

In Table 3 we compare several theoretical ${}^6_\Lambda\text{H}$ predictions to each other and to FINUDA's findings. The table makes it clear that FINUDA's results do not support Akaishi's predictions according to which the two p -shell neutrons in ${}^6_\Lambda\text{H}$ enhance the $\Lambda\Sigma$ coupling contribution in ${}^4_\Lambda\text{H}$, thereby pushing down

Table 3: ${}^6_{\Lambda}\text{H}(0^+_{\text{g.s.}})$ binding energies $B_{2n/\Lambda}$ and doublet spacing $\Delta E(1^+_{\text{exc.}} - 0^+_{\text{g.s.}})$ predictions vs. experiment. E_{2n} marks the assumed ${}^5\text{H}$ resonance position w.r.t. $2n$ emission.

B & ΔE (MeV)	Akaishi		shell model	Hiyama	FINUDA
	[5]	[13]	this work	[20]	exp. [3, 4]
$E_{2n}({}^5\text{H})$	2.1	1.7	1.7	1.6	—
$B_{2n}({}^6_{\Lambda}\text{H})$	1.7	2.1	0.3	−1.1	0.8 ± 1.2
$B_{\Lambda}({}^6_{\Lambda}\text{H})$	5.8	5.8	4.0	2.5	4.5 ± 1.2
$\Delta E({}^6_{\Lambda}\text{H})$	2.4	2.4	1.2	—	1.0 ± 0.7

the ${}^6_{\Lambda}\text{H}(0^+_{\text{g.s.}})$ level by twice as much as it does in ${}^4_{\Lambda}\text{H}$ and thus doubling the $0^+_{\text{g.s.}} - 1^+_{\text{exc.}}$ spacing. In contrast to an overbound ${}^6_{\Lambda}\text{H}$ in Akaishi’s calculations, the ${}^3\text{H}-n-n-\Lambda$ four-body calculation by Hiyama et al. [20] does not bind ${}^6_{\Lambda}\text{H}$. This calculation is the only one that considers the ${}^5\text{H}$ core as a ${}^3\text{H}-n-n$ resonance, but then it disregards $\Lambda\Sigma$ coupling which is inexcusable in a few-body system whose lowest particle-stability threshold involves ${}^4_{\Lambda}\text{H}$. Our own shell-model estimate, allowing for a spatially extended $2n$ cluster, suggests a weakly bound ${}^6_{\Lambda}\text{H}(0^+_{\text{g.s.}})$ and a particle-unstable ${}^6_{\Lambda}\text{H}(1^+_{\text{exc.}})$ that decays only by emitting a low-energy neutron pair:

$${}^6_{\Lambda}\text{H}(1^+_{\text{exc.}}) \rightarrow {}^4_{\Lambda}\text{H}(0^+_{\text{g.s.}}) + 2n. \quad (5)$$

However, this decay is substantially suppressed both kinematically and dynamically, kinematically since s -wave emission requires a 3S_1 dineutron configuration which is Pauli-forbidden, and the allowed p -wave emission which is kinematically suppressed at low energy requires that *both* ${}^6_{\Lambda}\text{H}$ constituents, ${}^4_{\Lambda}\text{H}$ and $2n$, flip their Pauli spin which is disfavored dynamically. This leaves open the possibility that $M1$ γ emission to ${}^6_{\Lambda}\text{H}(0^+_{\text{g.s.}})$ provides a competitive decay mode of the $1^+_{\text{exc.}}$ level.

4. Neutron-rich hypernuclei beyond ${}^6_{\Lambda}\text{H}$

In the first part of this section we consider neutron-rich Λ hypernuclei that can be produced in double-charge exchange reactions (π^-, K^+) or (K^-, π^+) on stable nuclear targets in the p shell. These are ${}^6_{\Lambda}\text{H}$, which was discussed in the previous section, ${}^9_{\Lambda}\text{He}$, ${}^{10}_{\Lambda}\text{Li}$, ${}^{12}_{\Lambda}\text{Be}$, and ${}^{14}_{\Lambda}\text{B}$, with targets ${}^6\text{Li}$, ${}^9\text{Be}$, ${}^{10}\text{B}$, ${}^{12}\text{C}$, and ${}^{14}\text{N}$, respectively. In distinction from the unbound-core ${}^6_{\Lambda}\text{H}$,

all other neutron-rich Λ hypernuclei listed above are based on bound nuclear cores, which ensures their particle stability together with that of a few excited states. In the second half of the present section we outline the evaluation of $\Lambda\Sigma$ coupling matrix elements in heavier nuclear cores with substantial neutron excess, ^{48}Ca and ^{208}Pb .

4.1. *p*-shell neutron-rich hypernuclei beyond $^6_\Lambda\text{H}$

Table 4: Beyond-mean-field $\Delta B_\Lambda^{\text{g.s.}}$ shell-model contributions to normal-parity ground states of neutron-rich hypernuclei (in MeV); see text. ME stands for “matrix element”.

target AZ	n -rich $^A_\Lambda(Z-2)$	ME diag.	$\Lambda\Sigma$ diag.	$\Lambda\Sigma$ total	induced $\vec{l}_N \cdot \vec{s}_N$	$\Delta B_\Lambda^{\text{g.s.}}$ total
^9Be	$^9_\Lambda\text{He}(\frac{1}{2}^+)$	4.101	0.210	0.253	0.619	0.879
^{10}B	$^{10}_\Lambda\text{Li}(1^-)$	4.023	0.202	0.275	0.595	1.022
^{12}C	$^{12}_\Lambda\text{Be}(0^-)$	3.835	0.184	0.158	0.554	0.748
^{14}N	$^{14}_\Lambda\text{B}(1^-)$	3.884	0.189	0.255	0.458	0.785

In Table 4, we focus on $\Lambda\Sigma$ contributions to binding energies of normal-parity g.s. in neutron-rich *p*-shell hypernuclei.² Column 3 gives the diagonal matrix-element (ME) from the central components $\bar{V}_{\Lambda\Sigma}^{0p}$ and $\Delta_{\Lambda\Sigma}^{0p}$ of the coherent $\Lambda\Sigma$ coupling interaction. The contribution from $\bar{V}_{\Lambda\Sigma}^{0p}$ is given by Eq. (2), saturating this diagonal matrix element in $^9_\Lambda\text{He}$ and dominating it with a value 3.242 MeV in the other cases. Column 4 gives the corresponding downward energy shift $(\text{ME})^2/80$ assuming a constant 80 MeV separation between Λ and Σ states, and column 5 gives the energy shift in the full shell-model calculation, including contributions from nondiagonal matrix elements. We note that the total $\Lambda\Sigma$ contribution listed in column 5 agrees for $^{10}_\Lambda\text{Li}$ with that computed in Ref. [21] using the same YN shell-model interactions. More recently, these authors discussed $\Lambda\Sigma$ coupling effects on g.s. doublet spacings in $^{7-10}_\Lambda\text{Li}$ isotopes, obtaining moderate enhancements between 70 to 150

²We excluded $^{16}_\Lambda\text{C}$ which can be produced on ^{16}O target because its analysis involves $0s_\Lambda(1s-0d)_N$ matrix elements which are not constrained by any hypernuclear datum. For the same reason we ignored for $^{12}_\Lambda\text{Be}$ the positive-parity doublet built on $^{11}\text{Be}_{\text{g.s.}}(\frac{1}{2}^+)$, considering only the normal-parity doublet based on the $\frac{1}{2}^-$ excited state at 0.32 MeV.

keV [16]. We have reached similar conclusions for all the neutron-rich hypernuclei considered in the present work beyond ${}^6_\Lambda\text{H}$. We also note that a result very close to the total $\Lambda\Sigma$ coupling contribution is obtained using just the central $\Lambda\Sigma$ coupling interaction, except for ${}^{12}_\Lambda\text{Be}$ where the decreased shift in the complete calculation is due to the contribution of the non-central components to the diagonal matrix element. Generally, however, the increased energy shift beyond the diagonal contribution arises from Σ core states connected to the Λ core state by Gamow-Teller transitions. The shift gets smaller with increased fragmentation of the Gamow-Teller strength.

The total $\Lambda\Sigma$ contribution discussed above is only one component of the total beyond-mean-field (BMF) contribution $\Delta B_\Lambda^{\text{g.s.}}$. To obtain the latter, various spin-dependent ΛN contributions generated by $V_{\Lambda N}$ have to be added to the total $\Lambda\Sigma$ contributions listed in column 5 of Table 4. Column 6 lists one such spin-dependent ΛN contribution, arising from the Λ -induced $\vec{l}_N \cdot \vec{s}_N$ nuclear spin-orbit term of Eq. (1). By comparing column 5 with column 6, and both with the total BMF contributions listed in column 7, the last one, it is concluded that the majority of the BMF contributions arise from ΛN spin-dependent terms, dominated by $\vec{l}_N \cdot \vec{s}_N$.

Table 5: Binding energy predictions for neutron-rich p -shell hypernuclei (in MeV).

n -rich ${}^A_\Lambda Z$	normal ${}^A_\Lambda Z'$	normal $B_\Lambda^{\text{g.s.}}$	normal $\Delta B_\Lambda^{\text{g.s.}}$	n -rich $\Delta B_\Lambda^{\text{g.s.}}$	n -rich $B_\Lambda^{\text{g.s.}}$
${}^9_\Lambda\text{He}(\frac{1}{2}^+)$	${}^9_\Lambda\text{Li}/{}^9_\Lambda\text{B}$	8.44 ± 0.10	0.952	0.879	8.37 ± 0.10
${}^{10}_\Lambda\text{Li}(1^-)$	${}^{10}_\Lambda\text{Be}/{}^{10}_\Lambda\text{B}$	8.94 ± 0.11	0.518	1.022	9.44 ± 0.11
${}^{12}_\Lambda\text{Be}(0^-)$	${}^{12}_\Lambda\text{B}$	11.37 ± 0.06	0.869	0.748	11.25 ± 0.06
${}^{14}_\Lambda\text{B}(1^-)$	${}^{14}_\Lambda\text{C}$	12.17 ± 0.33	0.904	0.785	12.05 ± 0.33

Our Λ binding energy predictions for ground states of neutron-rich hypernuclei ${}^A_\Lambda Z$ in the p shell are summarized in the last column of Table 5. We used the experimentally known g.s. binding energies of same- A normal hypernuclei ${}^A_\Lambda Z'$ with $Z' > Z$ from [2], averaging statistically when necessary. The BMF contributions $\Delta B_\Lambda^{\text{g.s.}}$ (normal) to the binding energies of the ${}^A_\Lambda Z'$ ‘normal’ hypernuclei, taken from [10], are listed in column 3 and the BMF contributions $\Delta B_\Lambda^{\text{g.s.}}$ (n -rich) to the binding energies of the ${}^A_\Lambda Z$ neutron-rich hypernuclei value, which are reproduced in the last column of Table 4, are listed here in column 4. Finally, the predicted binding energies $B_\Lambda^{\text{g.s.}}$ (n -rich)

of the neutron-rich hypernuclei ${}^A_\Lambda Z$ are listed in the last column of Table 5, were evaluated according to

$$B_\Lambda^{\text{g.s.}}({}^A_\Lambda Z) = B_\Lambda^{\text{g.s.}}({}^A_\Lambda Z') - \Delta B_\Lambda^{\text{g.s.}}({}^A_\Lambda Z') + \Delta B_\Lambda^{\text{g.s.}}({}^A_\Lambda Z). \quad (6)$$

The resulting binding energies are lower by about 0.1 MeV than those of the corresponding normal hypernuclei, except for ${}^{10}_\Lambda\text{Li}$ with binding energy about 0.5 MeV *larger* than that of ${}^{10}\text{Be}$ – ${}^{10}_\Lambda\text{B}$.

The relatively small effects induced by the $\Lambda\Sigma$ coupling interaction on $B_\Lambda^{\text{g.s.}}$ persist also in the particle-stable portion of neutron-rich Λ hypernuclear spectra. Here we only mention that, except for ${}^{12}_\Lambda\text{Be}$, one anticipates a clear separation about or exceeding 3 MeV between g.s. (in ${}^9_\Lambda\text{He}$) or g.s.-doublet (in ${}^{10}_\Lambda\text{Li}$ and ${}^{14}_\Lambda\text{B}$) and the first-excited hypernuclear doublet. Thus, the g.s. or its doublet are likely to be observed in experimental searches of neutron-rich Λ hypernuclei using ${}^9\text{Be}$, ${}^{10}\text{B}$, and ${}^{14}\text{N}$ targets, provided a resolution of better than 2 MeV can be reached.

4.2. Medium weight and heavy hypernuclei

It was demonstrated in the previous subsection that the $\Lambda\Sigma$ coupling contributions to p -shell hypernuclear binding energies are considerably smaller than for the s -shell $A = 4$ hypernuclei. The underlying $\Lambda\Sigma$ matrix elements decrease by roughly factor of two upon going from the s -shell to the p -shell, and the resulting energy contributions roughly by factor of four. This trend persists upon going to heavier hypernuclei and, as shown below, it more than compensates for the larger $N - Z$ neutron excess available in heavier hypernuclei. To demonstrate how it works, we outline schematic shell-model weak-coupling calculations using G -matrix $\Lambda\Sigma$ central interactions generated from the NSC97f YN potential model by Halderson [22], with input and results listed in Table 6 across the periodic table. We note that although the separate contributions $\Lambda\Sigma(\bar{V})$ and $\Lambda\Sigma(\Delta)$ in ${}^9_\Lambda\text{He}$ differ from those using the Akaishi interaction (see Table 4), the summed $\Lambda\Sigma$ contribution is the same to within 2%. For ${}^{49}_\Lambda\text{Ca}$, its ${}^{48}\text{Ca}$ core consists of $0s, 0p, 1s - 0d$ closed shells of protons and neutrons, plus a closed $0f_{7/2}$ neutron shell with isospin $T = 4$. The required $0s_\Lambda 0f_N \leftrightarrow 0s_\Sigma 0f_N$ radial integrals are computed for HO $n\ell_N$ radial wavefunctions with $\hbar\omega = 45A^{-1/3} - 25A^{-2/3}$ MeV and are compared in the table to the $0s_\Lambda 0p_N \leftrightarrow 0s_\Sigma 0p_N$ radial integrals for ${}^9_\Lambda\text{He}$. The decrease in the values of $\bar{V}_{\Lambda\Sigma}$ and of $\Delta_{\Lambda\Sigma}$ upon going from ${}^9_\Lambda\text{He}$ to ${}^{49}_\Lambda\text{Ca}$ is remarkable, reflecting the poorer overlap between the hyperon $0s_Y$ and the nucleon

$0\ell_N$ radial wavefunctions as ℓ_N increases. The resulting $\Lambda\Sigma$ contributions to the binding energy are given separately for the Fermi spin-independent interaction using the listed values of $\bar{V}_{\Lambda\Sigma}$, and for the GT spin-dependent interaction using the listed values of $\Delta_{\Lambda\Sigma}$. The Fermi contribution involves a $0^+ \rightarrow 0^+$ core transition preserving the value of T , see Eq. (2). The GT contribution consists of three separate $0^+ \rightarrow 1^+$ core transitions of comparable strengths, transforming a $f_{7/2}$ neutron to (i) $f_{7/2}$ nucleon with nuclear-core isospin $T_N = 3$, or to $f_{5/2}$ nucleon with (ii) $T_N = 3$ or (iii) $T_N = 4$. The overall $\Lambda\Sigma$ contribution of 24 keV in $^{49}_{\Lambda}\text{Ca}$ is rather weak, one order of magnitude smaller than in $^9_{\Lambda}\text{He}$.

Table 6: $\Lambda\Sigma$ matrix elements and contributions to binding energies (in MeV) for neutron-rich hypernuclei across the periodic table, using NSC97f YN interactions from Halderson [22]. In all cases, the diagonal matrix element is given by $\sqrt{(T+1)/3T} \sum_{nlj} (2j+1) \bar{V}_{\Lambda\Sigma}^{nl_N}$, where the sum runs over orbits in the neutron excess.

$N-Z$	$^A_{\Lambda}Z$	$\bar{V}_{\Lambda\Sigma}$	$\Lambda\Sigma(\bar{V})$	$\Delta_{\Lambda\Sigma}$	$\Lambda\Sigma(\Delta)$	$\Delta B_{\Lambda}^{\text{g.s.}}(\Lambda\Sigma)$
4	$^9_{\Lambda}\text{He}$	1.194	0.143	4.070	0.104	0.246
8	$^{49}_{\Lambda}\text{Ca}$	0.175	0.010	0.946	0.014	0.024
22	$^{209}_{\Lambda}\text{Pb}$	0.0788	0.052	0.132	0.001	0.053

In $^{209}_{\Lambda}\text{Pb}$, the 44 excess neutrons run over the $2p$, $1f$, $0h_{9/2}$ and $0i_{13/2}$ orbits. The Fermi $0^+ \rightarrow 0^+$ core transition is calculated using Eq. (2) where, again, $\bar{V}_{\Lambda\Sigma}$ (with a value listed in Table 6) stands for the $(2j+1)$ average of the separate neutron-excess $\bar{V}_{\Lambda\Sigma}^{nl_N}$ radial integrals, resulting in a $\Lambda\Sigma$ contribution of merely 52 keV to the binding energy of $^{209}_{\Lambda}\text{Pb}$. For the calculation of the GT $0^+ \rightarrow 1^+$ core transitions, we define $\Delta_{\Lambda\Sigma}$ as a $(2j+1)$ average of $\Delta_{\Lambda\Sigma}^{nl_N}$ radial integrals over the neutron-excess incomplete LS shells $0h_{9/2}$ and $0i_{13/2}$ (with a value listed in the table). These are the neutron orbits that initiate the GT core transitions required in $^{209}_{\Lambda}\text{Pb}$, with structure similar to that encountered in $^{49}_{\Lambda}\text{Ca}$ for the $0f_{7/2}$ neutron orbit; details will be given elsewhere, suffice to say here that neither of these transitions results in a $\Lambda\Sigma$ contribution larger than 0.2 keV to the binding energy of $^{209}_{\Lambda}\text{Pb}$.

5. Summary and outlook

In this Letter we have presented detailed shell-model calculations of p -shell neutron-rich Λ hypernuclei using (i) ΛN effective interactions derived

by fitting to comprehensive γ -ray hypernuclear data, and (ii) theoretically motivated $\Lambda\Sigma$ interaction terms. None of the large effects conjectured by Akaishi and Yamazaki [5] to arise from $\Lambda\Sigma$ coherent coupling in neutron-rich hypernuclei is borne out by these realistic shell-model calculations. This is evident from the relatively modest $\Lambda\Sigma$ component of the total BMF contribution to the Λ hypernuclear g.s. binding-energy, marked $\Delta B_{\Lambda}^{\text{g.s.}}$ in Table 4. It should be emphasized, however, that $\Lambda\Sigma$ coupling plays an important role in doublet spacings in p -shell hypernuclei [10], just as it does for ${}^4_{\Lambda}\text{H}$ and ${}^4_{\Lambda}\text{He}$ [6]. Although the ground-state doublet spacings in ${}^{10}_{\Lambda}\text{Li}$ and ${}^{14}_{\Lambda}\text{B}$ probably can't be measured, $\Lambda\Sigma$ coupling contributes 40% and 55% to the predicted doublet spacings of 341 and 173 keV, respectively (as for ${}^{16}_{\Lambda}\text{O}$ [10], the ${}^{12}_{\Lambda}\text{Be}$ doublet spacing is predicted to be very small).

We have also discussed in detail the shell-model argumentation for a particle-stable ${}^6_{\Lambda}\text{H}$, comparing it with both Akaishi's prediction that overbinds ${}^6_{\Lambda}\text{H}$ and with a very recent four-body calculation by Hiyama and collaborators that finds it particle-unstable [20]. In Akaishi's case, we have argued that the effects of $\Lambda\Sigma$ coupling in ${}^6_{\Lambda}\text{H}$ cannot be very much larger than they are in ${}^4_{\Lambda}\text{H}$, whereas such effects are missing in Hiyama's calculation. Forthcoming experiments searching for neutron-rich Λ hypernuclei at J-PARC will shed more light on the $N - Z$ dependence of hypernuclear binding energies. Given the regularity of hypernuclear binding energies of heavy Λ hypernuclei with respect to those in light and medium-weight hypernuclei, as manifest in SHF-motivated density-dependent calculations [23] and in RMF calculations [24] extending over the whole periodic table, no strong phenomenological motivation exists to argue for substantial $N - Z$ effects in Λ hypernuclei. Indeed, this was demonstrated in the calculation outlined in the previous section for ${}^{49}_{\Lambda}\text{Ca}$ and ${}^{209}_{\Lambda}\text{Pb}$.

Acknowledgements

D.J.M. acknowledges the support by the U.S. DOE under Contract DE-AC02-98CH10886 with the Brookhaven National Laboratory, and A.G. acknowledges support by the EU initiative FP7, HadronPhysics3, under the SPHERE and LEANNIS cooperation programs.

References

- [1] R.H. Dalitz, R. Levi Setti, Nuovo Cimento 30 (1963) 489.

- [2] D.H. Davis, Nucl. Phys. A 754 (2005) 3c, and references listed therein, particularly D.H. Davis, J. Pniewski, Contemp. Phys. 27 (1986) 91.
- [3] M. Agnello, et al. (FINUDA Collab. + A. Gal), Phys. Rev. Lett. 108 (2012) 042501.
- [4] M. Agnello, et al. (FINUDA Collab. + A. Gal), Nucl. Phys. A 881 (2012) 269.
- [5] Y. Akaishi, T. Yamazaki, in *Physics and Detectors for DAΦNE*, Eds. S. Bianco et al., Frascati Physics Series Vol. XVI (INFN, Frascati, 1999) pp. 59-74.
- [6] Y. Akaishi, T. Harada, S. Shinmura, K.S. Myint, Phys. Rev. Lett. 84 (2000) 3539.
- [7] H. Nemura, Y. Akaishi, Y. Suzuki, Phys. Rev. Lett. 89 (2002) 142504.
- [8] S. Shinmura, K.S. Myint, T. Harada, Y. Akaishi, J. Phys. G 28 (2002) L1, and a revised calculation by S. Shinmura, et al., Mod. Phys. Lett. A 18 (2003) 128.
- [9] T. Takahashi, Nucl. Phys. A (HYP2012 Proc. in press); J-PARC E10, http://j-parc.jp/researcher/Hadron/en/Proposal_e.html.
- [10] D.J. Millener, Nucl. Phys. A 881 (2012) 298, and references therein.
- [11] H. Tamura, et al., Nucl. Phys. A 835 (2010) 3, and references therein.
- [12] K.S. Myint, Y. Akaishi, Prog. Theor. Phys. Suppl. 146 (2002) 599.
- [13] Y. Akaishi, K.S. Myint, AIP Conf. Proc. 1011 (2008) 277.
- [14] D.J. Millener, Nucl. Phys. A 835 (2010) 11.
- [15] Th.A. Rijken, V.J.G. Stoks, Y. Yamamoto, Phys. Rev. C 59 (1999) 21.
- [16] A. Umeya, T. Harada, Phys. Rev. C 83 (2011) 034310.
- [17] H. Tamura, et al., Nucl. Phys. A 881 (2012) 310, and references therein.
- [18] A.A. Korshennikov, et al., Phys. Rev. Lett. 87 (2001) 092501.

- [19] S.N. Nakamura, et al. (JLab E01-011), Phys. Rev. Lett. 110 (2013) 012502.
- [20] E. Hiyama, S. Ohnishi, M. Kamimura, Y. Yamamoto, Nucl. Phys. A 908 (2013) 29.
- [21] A. Umeya, T. Harada, Phys. Rev. C 79 (2009) 024315.
- [22] D. Halderson, private communication.
- [23] D.J. Millener, C.B. Dover, A. Gal, Phys. Rev. C 38 (1988) 2700.
- [24] J. Mareš, B.K. Jennings, Phys. Rev. C 49 (1994) 2472.